Functional Surfaces with Photocatalytic Behavior and Reversible Wettability: ZnO Coating on Silicon Spikes
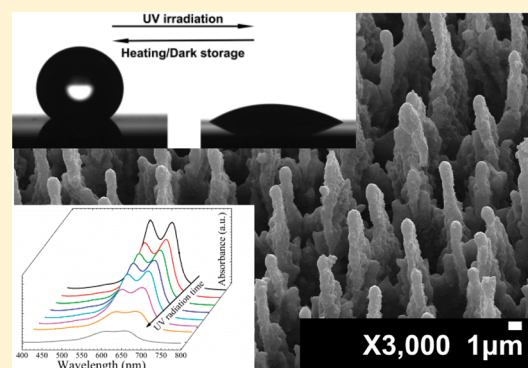
Melani A. Frysali,[†,‡] Lampros Papoutsakis,[†] George Kenanakis,[†] and Spiros H. Anastasiadis*[,†,‡]

[†]Institute of Electronic Structure and Laser, Foundation for Research and Technology - Hellas, P.O. Box 1385, 711 10 Heraklion, Crete, Greece

[‡]Department of Chemistry, University of Crete, P.O. Box 2208, 710 03 Heraklion, Crete, Greece

ABSTRACT: Multifunctional surfaces with reversible characteristics have gained great attention due to their various envisioned applications. We report on the development of surfaces exhibiting both photocatalytic activity and reversible wettability. Initially, irradiation of silicon wafers with femtosecond laser pulses produces a surface with dual-scale roughness in the micro- and nanoscale. Subsequently, the hierarchically roughened silicon surfaces are coated with ZnO following a simple sol–gel process. The manufactured artificial surfaces exhibit reversible wettability from superhydrophilic (upon UV irradiation) to superhydrophobic (upon heating), while the specimens reveal high photocatalytic activity as illustrated by the decolorization of methylene blue utilized as a model dye. The surfaces exhibit reproducibility and stability over a number of cycles.

I. INTRODUCTION

Self-cleaning surfaces have gained the focus of considerable research due to their strong potential for exploitation in a number of industrial applications.[1] Superhydrophobic materials can be widely used in outdoor weather-proof paints, easy-to-clean textiles, microfluidics, lab-on-chip devices, low friction coatings (e.g., for ships), and solar panels. In most cases, when superhydrophobicity is discussed, one means surfaces with high contact angles (>150°) and low contact angle hysteresis (or sliding angles) with water droplets being able to roll off easily from the surfaces;[2−6] in those cases, the surfaces exhibit water repellency[3−5,7−9] and are frequently described as superhydrophobic with low adhesion. However, there are many naturally occurring surfaces that exhibit high contact angles (>150°) together with high contact angle hysteresis (>90°); these surfaces are called superhydrophobic with high adhesion.[10−12] As the flip side of the coin, superhydrophilic surfaces are used in the cleaning of roof tiles and windows, in mist-free mirrors, and in photochemical degradation, to name but a few applications.[13] The inspiration for designing and developing new self-cleaning materials comes from nature;[1] the Lotus effect, which results in superhydrophobicity and very high water repellency, as exhibited by the leaves of sacred Lotus (Nelumbo nucifera), was first reported by Barthlott and Neinhuis.[14,15] Apart from this, there is a wide variety of biological species exhibiting amazing properties, like rice leaves, rose petals, the strider's legs, gecko feet, shark skin, mosquito compound eye, spider silks, and cicada and butterfly wings.[16]

The most common way to generate effective superhydrophobic surfaces is to build multiscale hierarchical roughness. One way this can be achieved is by micro/nanostructruring a surface utilizing ultrafast lasers, which creates dual scale roughness in a one-step process.[3,17] The first conical microstructures with multiscale roughness were reported by Her and Mazur[18] in 1998. Since then, femtosecond laser has proven to be a promising method for fabricating hierarchical structures with multiscale roughness.[19] For example, Zorba et al. produced artificially structured surfaces possessing controlled dual-scale roughness, which exhibited the water repellent characteristics of the natural Lotus leaf.[3,20,21]

Moreover, there is a continuously increasing demand for multifunctional surfaces with reversible characteristics. This can be achieved by using "smart" coatings, which can respond to external stimuli, such as light,[22−26] temperature,[22,27−29] electric field,[22,29−31] pH,[22,32−34] or solvent selectivity.[22,34] Among them, the wetting properties of ZnO have been widely studied, since it can reversibly switch from superhydrophilic to superhydrophobic in response to UV irradiation and heating or dark storage, respectively.[35−37] For example, Papadopoulou et al. reported the preparation of photoreversible ZnO hierarchical surfaces prepared by irradiating Si substrates with femtosecond laser and decorating them with ZnO nano-protrusions using pulsed laser deposition.[35]

Furthermore, ZnO is a well-known photocatalyst. In order to enhance its photocatalytic activity, research efforts have focused on the development of ZnO surfaces with a high surface to volume ratio. Among those, ZnO nanorods,[37,38] nanoflowers,[39] nanobelts, and nanowires[40] have been reported, which can be

Figure 1. AFM image (scan size 1 μm × 1 μm; z-range ~62 nm) (a) and X-ray diffractogram (b) of a ~80-nm-thick ZnO film on a flat silicon substrate.

easily produced by a simple sol−gel method followed by hydrothermal synthesis or other approaches.[37,41] However, most of the work cited above suffers from the disadvantage of producing low stability specimens, which cannot be easily adopted for large-scale synthesis and, thus, for industrial applications.

The research efforts up to now have focused on either superhydrophobic photocatalytic ZnO surfaces or superhydrophilic photocatalytic self-cleaning surfaces. The combination of surfaces exhibiting reversible wettability behavior (from superhydrophobic to superhydrophilic) together with excellent photocatalytic activity is an innovative point of view, since such smart surfaces can reduce the maintenance costs and save time. In this work, we report the development of ZnO coatings exhibiting reversible wettability and photocatalytic activity. These are prepared following a two-step fabrication process. First, silicon (Si) wafers are irradiated with femtosecond (fs) laser pulses in order to produce Si surfaces with dual scale roughness (Si spikes).[3,20,21] Then, the rough Si samples are coated with a ZnO film prepared by a simple sol−gel process.[41−43] The artificial surfaces exhibit reversible wettability from superhydrophilic (upon UV irradiation) to superhydrophobic (upon heating), while the as-grown samples revealed high photocatalytic activity investigated by means of the decolorization of methylene blue as a model dye. The reproducibility and sustainability of the system is thoroughly studied. To the best of our knowledge, this is the first investigation referring to ZnO surfaces on Si spikes, which illustrate both high photocatalytic activity and reversible wettability from superhydrophobic to superhydrophilic.

II. EXPERIMENTAL SECTION

Surface Manufacturing. The fabrication of Si spikes with a ZnO coating was achieved following a two-step process: First, single crystal *n*-type Si (100) wafers with a resistivity of $\rho = 2-8$ Ω·cm were placed in a vacuum chamber under a pressure of 10^{-2} mbar (which is drained with a reactive gas (SF_6) atmosphere at a pressure of 500 Torr) and irradiated using a Yb:KGW laser with a repetition rate of 1 kHz and a pulse duration of 170 fs at a wavelength of 1026 nm, while the laser

pulse fluence was maintained at 0.65 J/cm². The chamber was mounted on a high precision X−Y translational stage and the sample surface was kept perpendicular to the incident laser beam. The stage motion was synchronized with a mechanical shutter in order to provide a uniform exposure of a 100 mm² area to an average of 500 laser pulses per spot. After that, the samples were cleaned with a 10% HF aqueous solutions in order to remove the silicon oxide grown on the surface.[3,20,21]

After rinsing several times with ethanol and bidistilled water in order to remove any remains, the surfaces were coated by a ZnO film using a simple sol−gel process.[41−43] For this purpose, Zinc acetate dihydrate [(Zn(CH₂COO)₂·2H₂O), Sigma-Aldrich, 99.99%] was dissolved in 2-methoxy ethanol [(CH₃OCH₂CH₂OH), Sigma-Aldrich, ≥99.55%] at a concentration of 0.75 mol/L. Monoethanolamine [(HOCH₂CH₂NH₂), Sigma-Aldrich, ≥99.0%] was also added as a stabilizer and the molar ratio of zinc acetate to ethanolamine was kept at 1:1. The resultant solution was stirred for 1 h at 60 °C in order to become homogeneous. Subsequently, 30 μL of the solution were dropped on the laser irradiated Si samples, which were rotated at 3000 rpm for 20 s. After coating, the samples were heated at 350 °C for 10 min to evaporate the solvent and remove any organic residue. This procedure was repeated four (4×) times. Finally, the samples were annealed in air at 500 °C for 1 h. In parallel with the deposition of the ZnO coatings on Si spikes, ZnO films on flat silicon wafers were grown as well. This way, reference specimens of ZnO on flat silicon were created for reference and comparison reasons.

Surface Characterization. The surface morphology of flat Si substrates coated with ZnO films was investigated using an atomic force microscope (AFM) in tapping mode (Digital instruments - Nanoscope IIIa). The grain size and the roughness (rms) of the ZnO films on flat Si wafers were determined using the scanning probe image processing software (SPIP, v 3.3.5.0, Image Metrology) for nano- and microscale microscopy, while the thickness of the ZnO film was measured with a stylus profilometer (alpha-step 100, Tencor). The morphology of laser irradiated Si surfaces, with and without the ZnO coating, was studied using a field emission scanning
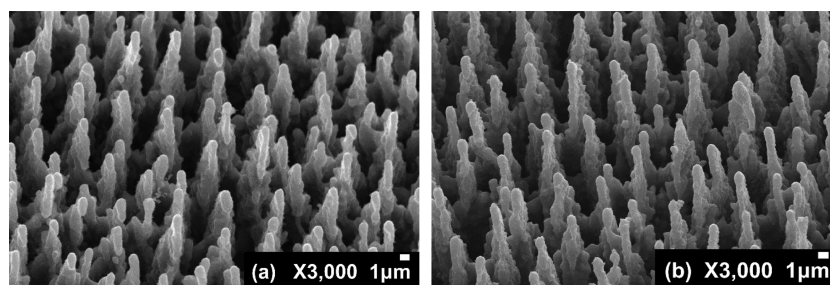
Figure 2. FE-SEM micrographs of bare Si spikes prepared by femtosecond laser irradiation on silicon (a) and coated with ZnO by the sol−gel/spin-coating process (b).
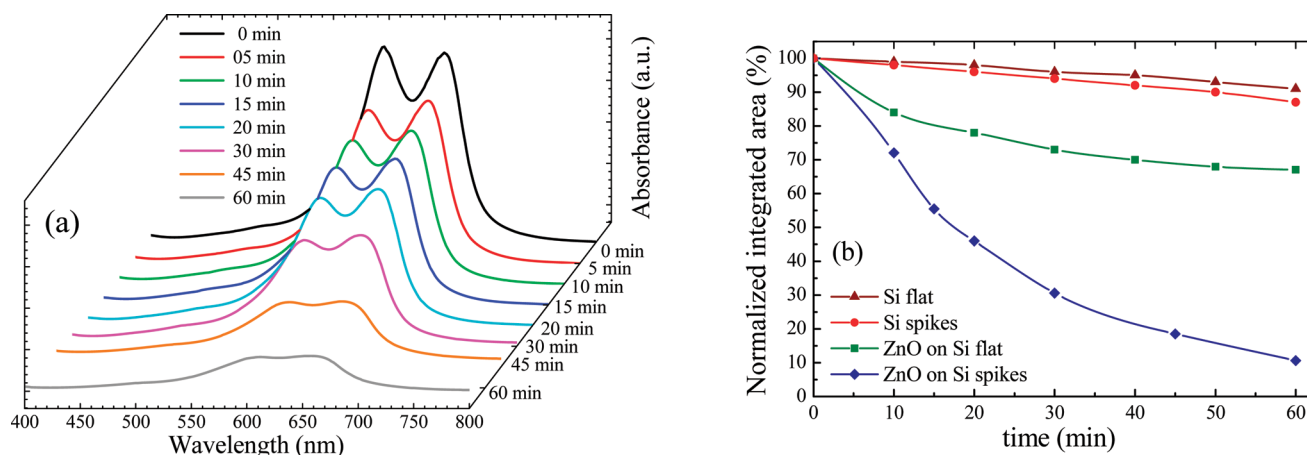

Figure 3. (a) UV−vis absorption spectra of aqueous solution of methylene blue in contact with a surface with a ZnO coating on top of silicon spikes following UV irradiation for various times. (b) Normalized absorption of aqueous solutions of methylene blue at λ_{max} = 665 nm under UV light irradiation, for flat Si substrate (triangles), Si spikes (circles), 4× ZnO coating on flat silicon (squares), and 4× ZnO coating on silicon spikes (diamonds), respectively.

electron microscope (FE-SEM, JEOL JSM-7000F), while the crystalline structure of all samples was determined by X-ray diffraction (XRD) utilizing a Rigaku (RINT 2000) diffractometer with Cu Kα radiation with a wavelength λ = 1.54 Å.

Photocatalysis. The photocatalytic activity of the samples was quantified by means of the decolorization of methylene blue (MB) in aqueous solution at an initial concentration of 5.4 × 10^{-7} mol/L (20 ppm), which is a typical potent cationic dye that has been widely used as a model organic probe to test the photocatalytic performance of photocatalysts.[44−47] The studied samples (both ZnO coated and bare Si spikes) were placed in a custom-made quartz cell, and the whole setup was illuminated for up to 60 min using a UV lamp centered at 365 nm (Philips HPK 125 W) with a light intensity of ~10 mW/cm^2. The MB concentration was monitored during decolorization by UV−vis spectroscopy in absorption mode, using a PerkinElmer (Lambda 950) spectrophotometer over the wavelength range of 250−1100 nm. In addition, an apparent rate constant (k) has been calculated as the basic kinetic parameter for the comparison of the photocatalytic activities. The rate constant k was obtained by fitting the concentration data to an equation

$$\ln(C_t/C_0) = -kt$$

where k is apparent rate constant, C_t is the actual concentration at time t, and C_0 the initial concentration of MB. Since methylene blue has a strong absorption peak at λ_{max} = 665 nm, a series of MB aqueous solutions of known concentration were prepared first in order to build a calibration curve. Photolysis experiments were also performed using bare Si substrates and

bare Si spikes, under exactly the same conditions applied for the ZnO coated surfaces.

Wettability. Wettability tests were performed using a surface tensiometer (OCA-40, Dataphysics) utilizing the sessile drop method.[48] A drop of 5 μL was deposited on the surface of each substrate after exposure to the UV lamp or heating at 200 °C and the contact angle was measured in each case. Digital images of the water droplets were taken and the water contact angle was calculated by fitting the whole drop profile using Bashforth-Adams equation, thus evaluating both the contact angle and the surface tension of the fluid.

III. RESULTS AND DISCUSSION

Artificial Surface Characterization. An AFM image of a 4× layered ZnO film on a flat Si wafer is shown in Figure 1a, with a scanned surface area of 1 μm^2. The thickness of the film was ~80 nm estimated with the stylus profilometer. The determined rms roughness of the film is ~9.5 nm while the grain size is estimated as ~36.5 ± 2 nm. Figure 1b depicts a typical X-ray diffraction pattern of the ZnO thin films deposited on silicon by the sol−gel/spin-coating technique after 4 spinning cycles and annealing at 500 °C. XRD pattern reveals a strong (002) peak at a diffraction angle of 2θ = 34.42° and two more at 31.78° and 16.20°, which correspond to the (100) and (101) planes, respectively, in good agreement with the JCPDS card (No. 36−1451) for a typical hexagonal wurtzite type ZnO crystal. No other characteristic peaks corresponding to possible impurities, such as zinc nitrate or zinc hydroxide, are observed in the XRD patterns.

Figure 2 shows the SEM micrographs of the laser irradiated Si substrates before and after the ZnO coating. Careful examination of Figure 2a and b makes clear that the ZnO coating did not affect the hierarchical micro- and nanostructure of the artificial surface; in both images, silicon spikes are clearly visible and distinct. This is reasonable since the roughness introduced by the ZnO layer is on the order of a few tens of nanometers while the spike dimensions are on the order of tens of microns (the peak of the spikes alone is close to 1 μm wide) and their nanoroughness is on the order of 100 nm. Therefore, the quantity of ZnO used is sufficient to create a very thin film on the surface of each spike but not in excess that would submerge them and make the roughness inefficient.

Photocatalytic Behavior. The photocatalytic mechanism of ZnO has been reported in previous works.[37,41,49] UV−vis spectroscopy was utilized to evaluate the photocatalytic behavior of the rough surfaces with the ZnO film coating as well as of the various controls. A custom-made cuvette was used that brought into contact the aqueous solution of methylene blue and the coated or noncoated surfaces during UV illumination. The absorbance as a function of wavelength for various UV illumination time intervals was monitored for each specimen; Figure 3a shows the absorption spectra for the specimen with the ZnO coating on top of the silicon spikes. The normalized integrated areas were calculated below such absorbance curves at the peak wavelength and the data are shown in Figure 3b as a function of the UV illumination time. Figure 3b illustrates the photocatalytic behavior of flat Si substrates, both bare and with a ZnO coating, along with the hierarchical surfaces (silicon spikes) both bare and with a ZnO coating.

The ZnO coated silicon spikes exhibit high photocatalytic activity when compared to a ZnO film on flat silicon. For the ZnO on the spikes, the degradation of MB reaches about 90% in only 60 min (even ∼70% degradation in only 30 min), while for a ZnO on flat silicon the degradation is only ∼30% after 60 min. This can be attributed to the high surface-to-volume ratio of the ZnO coated on the silicon spikes, in agreement with research results reported in the literature.[41,50,51] The integrated area is proportional to the MB concentration; thus, analysis of the data of Figure 3b with the equation

$$\ln(I_t/I_0) = \ln(C_t/C_0) = -kt$$

(see Experimental Section) can be used to extract an apparent rate constant. The data in Figure 3b (especially for the ZnO film on silicon spikes) give a good linear fit, thus confirming that the photodegradation of MB over the studied photocatalysts follows first-order kinetics. The calculated apparent rate constant for the ZnO coated silicon spikes was 0.016 min^{-1}, which is close to the values recorded in the literature.[42,52] Reference samples (flat Si substrate and Si spikes) without ZnO coatings were also characterized in terms of MB decolorization by means of UV−vis absorption and showed that their photocatalytic activity was negligible.

Reversible Wettability Behavior. Figure 4 shows representative water drop images for the specimen with a ZnO coating onto a flat silicon surface (Figure 4a) and onto a micro/nanostructured surface of silicon spikes (Figure 4b) following a cycle of UV irradiation and of subsequent heating. It can be clearly seen that, as the samples are exposed to UV illumination, they both become hydrophilic, while when the same samples are heated at 200 °C for 3 h, an increase in their contact angle is recorded. It should be noted that the
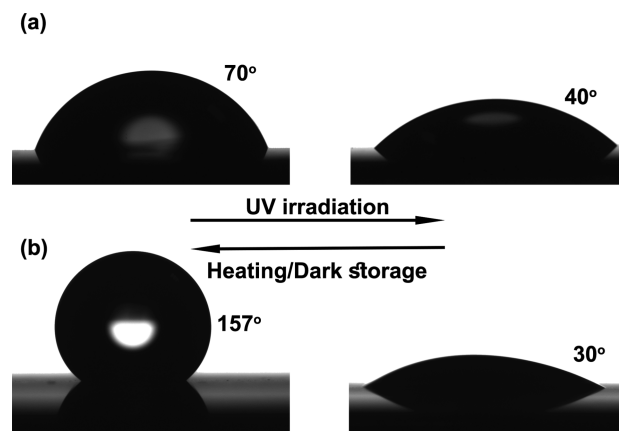

Figure 4. Photographs of representative water drops and the respective equilibrium contact angles on specimens with (a) ZnO coating onto a flat Si substrate and (b) ZnO coating onto a surface with silicon spikes. Drops are shown for the specimens following UV irradiation (on the right) and after thermal treatment at 200 °C (on the left).

hydrophobic behavior of the specimens can also be achieved by storing them in the dark, although this process requires time on the order of days.[35,36] The contact angle of water on the ZnO coated flat silicon surfaces is measured at ∼70° after heating while that on the ZnO coated silicon spikes gives values of ∼157°, illustrating their superhydrophobic behavior. The difference in the contact angle measurements between these two ZnO surfaces is due to the enhanced hierarchical roughness in the latter case. To the best of our knowledge, this is the first study presenting a superhydrophobic ZnO surface with a contact angle more than 150°. It is noted that our hierarchical surfaces did not exhibit low contact angle hysteresis (or, equivalently low sliding angle; data not shown). Water droplets stayed attached onto the surfaces even for angles as high as 90°. It is noted that the pinning force per unit length for a droplet on a surface is $F = \gamma_{LV}(\cos\theta_r - \cos\theta_a) = \gamma_{LV}\Delta(\cos\theta)$, with γ_{LV} the water surface tension and θ_a and θ_r the advancing and receding contact angles, respectively; the energy dissipated will, thus, scale as $\gamma_{LV}R^2\Delta(\cos\theta)$, with R the droplet radius.[8] Thus, our surfaces are superhydrophobic with high water adhesion, similar to a number of biosurfaces like, e.g., the Rosa, cv. Bairage.[12] This behavior indicates that the Si irradiated surfaces were not fully covered by the ZnO layers, which potentially could give space to the formation of hydrophilic defects that prevent droplets from rolling off.[10,11]

Figure 5 shows the water contact angles as a function of time of UV illumination (Figure 5a) and heating (Figure 5b), respectively, for a specimen with a ZnO coating onto a micro/nanostructured surface of silicon spikes. When the surface is illuminated with UV, the contact angle decreases slowly with time until it reaches the superhydrophilic regime after about 50 min. On the other hand, when the same surface is heated at 200 °C, an apparently two-stage process is observed. The contact angle increases at a faster rate for early times reaching ∼120° after ∼50 min whereas it, then, increases with a slower rate until it reaches a superhydrophobic state after ∼160 min of exposure to heat. Other temperatures were also tested. Lower temperatures caused a rapid decrease in efficiency while higher temperatures did not make the process much faster or more efficient. This makes the whole process affordable in energy
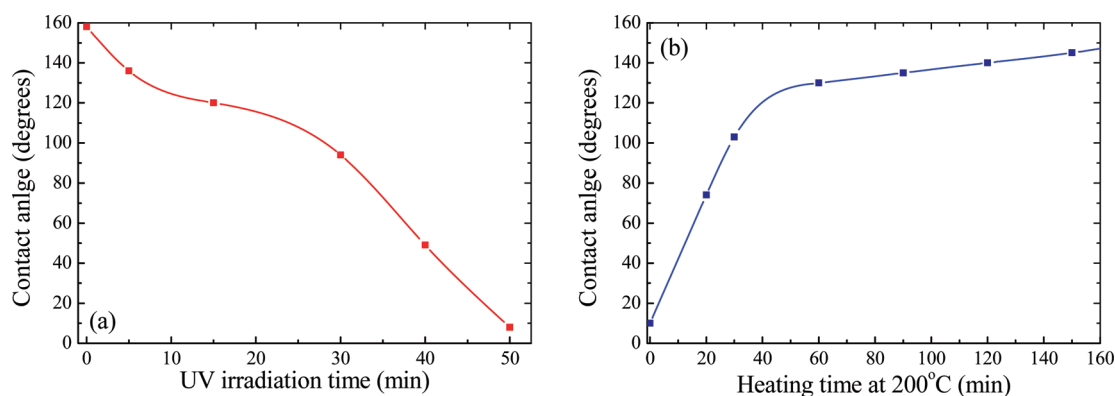
Figure 5. Dependence of the water contact angle on a surface with a ZnO coating on top of the silicon spikes following (a) UV irradiation and (b) heating at 200 °C for various times.

cost and convenient since it does not require any sophisticated equipment for heating.

Stability of the Behavior. In order to study the reproducibility and the stability of the system, specimens have been subjected to cycles of UV irradiation and thermal heating and their wettability is investigated (Figure 6). The
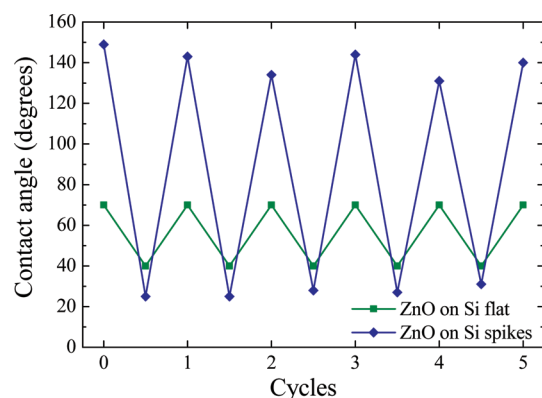

Figure 6. Average contact angle values of water droplets situated on specimens with ZnO coating onto a flat Si substrate (squares) and ZnO coating onto a surface with silicon spikes (diamonds) for five irradiation cycles of UV irradiation and 3 h thermal heating at 200 °C.

water contact angle data are shown for the specimens with a ZnO coating onto a surface with silicon spikes and the one with a ZnO coating onto a flat silicon substrate for five cycles of UV illumination and heating. A responsive behavior is observed for the case of the ZnO coated flat specimen with contact angle values fluctuating within a narrow region between 40° and 70°. On the contrary, the ZnO coated hierarchically roughened specimen exhibits a very wide range in responsiveness ranging from around 20° to a region very close to 150°. Both reversibility and reproducibility prove the efficiency and endurance of the surfaces, which is very important for practical applications.

It has been reported in the literature that there is a possibility for photocorrosion under UV irradiation of the ZnO catalyst;[49] this is more prone to happen for ultrathin (20−70 nm) films of ZnO. Thus, we have performed tests of the present system for the stability and reproducibility of the photocatalytic behavior. For that, cycles of both wettability and photocatalysis measurements were performed and the performance is illustrated in Table 1.

Table 1. Repeatability of the Specimen Performance

	wettability		photocatalysis		
			% degradation of methylene blue		
	after heating in 200 °C	after UV irradiation	after 20 min irradiation	after 60 min irradiation	reaction constant (k)
1st cycle	157°	10°	22	86	0.016 s⁻¹
2nd cycle	151°	20°	21	84	0.016 s⁻¹

According to the results the surface maintains the reversible wettability behavior after photocatalysis as well as its super-hydrophobic features. Furthermore, the second cycle of photocatalysis proved to be as efficient as the first one, without any reduction of the reaction rate constant. Therefore, the system maintained its efficiency after repeated wettability—photocatalysis cycles proving its reproducibility and stability. Such a biresponsive structure could be the basis for a variety of applications in the future.

IV. CONCLUSIONS

A multifunctional surface with a ZnO coating deposited onto a hierarchically roughened surface has been fabricated with a two-step process. The wettability and the photocatalytic activity of the surfaces have been investigated in detail as a function of time. High photocatalytic activity is achieved with a ∼90% decolorization of a model dye in ∼60 min. The systems exhibit a reversible wettability behavior from superhydrophilic (upon UV irradiation) to superhydrophobic (upon heating). The stability of the behavior is investigated extensively and the system proves to be quite stable. To the best of our knowledge, this is the first work on the development of surfaces with both high photocatalytic activity and reversible wettability behavior from superhydrophobic to superhydrophilic. The combination of photocatalysis with reversible wettability with a single coating makes the system appropriate for a variety of applications, such as self-cleaning surfaces, air purification, marine coatings, or fog-proofing.

■ AUTHOR INFORMATION

Corresponding Author
*E-mail: spiros@iesl.forth.gr. Phone: +30-2810-391466. Fax: +30-2810-391305.

Notes

■ ACKNOWLEDGMENTS

■ REFERENCES

(1) Anastasiadis, S. H. Development of Functional Polymer Surfaces with Controlled Wettability. *Langmuir* **2013**, *29*, 9277−9290.

(2) Bhushan, B.; Jung, Y. C.; Koch, K. Micro-, Nano- and Hierarchical Structures for Superhydrophobicity, Self-Cleaning and Low Adhesion. *Philos. Trans. R. Soc., A* **2009**, *367*, 1631−1672.

(3) Zorba, V.; Stratakis, E.; Barberoglou, M.; Spanakis, E.; Tzanetakis, P.; Anastasiadis, S. H.; Fotakis, C. Biomimetic Artificial Surfaces Quantitatively Reproduce the Water Repellency of a Lotus Leaf. *Adv. Mater.* **2008**, *20*, 4049−4054.

(4) Blossey, R. Self-Cleaning Surfaces–Virtual Realities. *Nat. Mater.* **2003**, *2*, 301−306.

(5) Callies, M.; Quéré, D. *Soft Matter* **2005**, *1*, 55.

(6) Nakajima, A.; Fujishima, A.; Hashimoto, K.; Watanabe, T. Preparation of Transparent Superhydrophobic Boehmite and Silica Films by Sublimation of Aluminum Acetylacetonate. *Adv. Mater.* **1999**, *11*, 1365−1368.

(7) Wang, B.-B.; Feng, J.-T.; Zhao, Y.-P.; Yu, T. X. Fabrication of Novel Superhydrophobic Surfaces and Water Droplet Bouncing Behavior — Part 1: Stable ZnO−PDMS Superhydrophobic Surface with Low Hysteresis Constructed Using ZnO Nanoparticles. *J. Adhes. Sci. Technol.* **2010**, *24*, 2693−2705.

(8) Wang, B.-B.; Zhao, Y.-P.; Yu, T. Fabrication of Novel Superhydrophobic Surfaces and Droplet Bouncing Behavior — Part 2: Water Droplet Impact Experiment on Superhydrophobic Surfaces Constructed Using ZnO Nanoparticles. *J. Adhes. Sci. Technol.* **2011**, *25*, 93−108.

(9) Wang, Z.; Wang, F.-C.; Zhao, Y.-P. Tap Dance of a Water Droplet. *Proc. R. Soc. London, Ser. A* **2012**, *468*, 2485−2495.

(10) Chang, F.-M.; Hong, S.-J.; Sheng, Y.-J.; Tsao, H.-K. High Contact Angle Hysteresis of Superhydrophobic Surfaces: Hydrophobic Defects. *Appl. Phys. Lett.* **2009**, *95*, 064102.

(11) Wang, L.; Wei, J.; Su, Z. Fabrication of Surfaces with Extremely High Contact Angle Hysteresis from Polyelectrolyte Multilayer. *Langmuir* **2011**, *27*, 15299−15304.

(12) Bhushan, B. Bioinspired Structured Surfaces. *Langmuir* **2012**, *28*, 1698−1714.

(13) Ueda, E.; Levkin, P. A. Emerging Applications of Superhydrophilic-Superhydrophobic Micropatterns. *Adv. Mater.* **2013**, *25*, 1234−1247.

(14) Barthlott, W.; Neinhuis, C. Purity of the Sacred Lotus, or Escape from Contamination in Biological Surfaces. *Planta* **1997**, *202*, 1−8.

(15) Fürstner, R.; Barthlott, W.; Neinhuis, C.; Walzel, P. Wetting and Self-Cleaning Properties of Artificial Superhydrophobic Surfaces. *Langmuir* **2005**, *21*, 956−961.

(16) Liu, K.; Jiang, L. Bio-Inspired Design of Multiscale Structures for Function Integration. *Nano Today* **2011**, *6*, 155−175.

(17) Hsu, S.-T.; Wang, H.; Satoh, G.; Yao, Y. L. Applications of Surface Structuring with Lasers. *Icaleo* **2011**, *1095−1104*.

(18) Her, T.-H.; Finlay, R. J.; Wu, C.; Deliwala, S.; Mazur, E. Microstructuring of Silicon with Femtosecond Laser Pulses. *Appl. Phys. Lett.* **1998**, *73*, 1673.

(19) Zhang, D.; Chen, F.; Yang, Q.; Yong, J.; Bian, H.; Ou, Y.; Si, J.; Meng, X.; Hou, X. A Simple Way to Achieve Pattern-Dependent Tunable Adhesion in Superhydrophobic Surfaces by a Femtosecond Laser. *ACS Appl. Mater. Interfaces* **2012**, *4*, 4905−4912.

(20) Zorba, V.; Persano, L.; Pisignano, D.; Athanassiou, a; Stratakis, E.; Cingolani, R.; Tzanetakis, P.; Fotakis, C. Making Silicon Hydrophobic: Wettability Control by Two-Lengthscale Simultaneous Patterning with Femtosecond Laser Irradiation. *Nanotechnology* **2006**, *17*, 3234−3238.

(21) Barberoglou, M.; Zorba, V.; Stratakis, E.; Spanakis, E.; Tzanetakis, P.; Anastasiadis, S. H.; Fotakis, C. Bio-Inspired Water Repellent Surfaces Produced by Ultrafast Laser Structuring of Silicon. *Appl. Surf. Sci.* **2009**, *255*, 5425−5429.

(22) Wang, S.; Song, Y.; Jiang, L. Photoresponsive Surfaces with Controllable Wettability. *J. Photochem. Photobiol., C* **2007**, *8*, 18−29.

(23) Feng, X.; Jiang, L. Design and Creation of Superwetting/antiwetting Surfaces. *Adv. Mater.* **2006**, *18*, 3063−3078.

(24) Rosario, R.; Gust, D.; Hayes, M.; Jahnke, F.; Springer, J.; Garcia, A. A. Photon-Modulated Wettability Changes on Spiropyran-Coated Surfaces. *Langmuir* **2002**, *18*, 8062−8069.

(25) Liu, H.; Feng, L.; Zhai, J.; Jiang, L.; Zhu, D. Reversible Wettability of a Chemical Vapor Deposition Prepared ZnO Film between Superhydrophobicity and Superhydrophilicity. *Langmuir* **2004**, *20*, 5659−5661.

(26) Irie, H.; Ping, T. S.; Shibata, T.; Hashimoto, K. Reversible Control of Wettability of a TiO[sub 2] Surface by Introducing Surface Roughness. *Electrochem. Solid-State Lett.* **2005**, *8*, D23.

(27) Crevoisier, G. D. Switchable Tackiness and Wettability of a Liquid Crystalline Polymer. *Science (Washington, DC, U. S.)* **1999**, *285*, 1246−1249.

(28) Fu, Q.; Rao, G. V. R.; Basame, S. B.; Keller, D. J.; Artyushkova, K.; Fulghum, J. E.; López, G. P. Reversible Control of Free Energy and Topography of Nanostructured Surfaces. *J. Am. Chem. Soc.* **2004**, *126*, 8904−8905.

(29) Sun, T.; Wang, G.; Feng, L.; Liu, B.; Ma, Y.; Jiang, L.; Zhu, D. Reversible Switching between Superhydrophilicity and Superhydrophobicity. *Angew. Chem., Int. Ed.* **2004**, *43*, 357−360.

(30) Lahann, J.; Mitragotri, S.; Tran, T.-N.; Kaido, H.; Sundaram, J.; Choi, I. S.; Hoffer, S.; Somorjai, G. A.; Langer, R. A Reversibly Switching Surface. *Science* **2003**, *299*, 371−374.

(31) Krupenkin, T. N.; Taylor, J. A.; Schneider, T. M.; Yang, S. From Rolling Ball to Complete Wetting: The Dynamic Tuning of Liquids on Nanostructured Surfaces. *Langmuir* **2004**, *20*, 3824−3827.

(32) Yu, X.; Wang, Z.; Jiang, Y.; Shi, F.; Zhang, X. Reversible pH-Responsive Surface: From Superhydrophobicity to Superhydrophilicity. *Adv. Mater.* **2005**, *17*, 1289−1293.

(33) Stratakis, E.; Mateescu, A.; Barberoglou, M.; Vamvakaki, M.; Fotakis, C.; Anastasiadis, S. H. From Superhydrophobicity and Water Repellency to Superhydrophilicity: Smart Polymer-Functionalized Surfaces. *Chem. Commun.* **2010**, *46*, 4136.

(34) Minko, S.; Müller, M.; Motornov, M.; Nitschke, M.; Grundke, K.; Stamm, M. Two-Level Structured Self-Adaptive Surfaces with Reversibly Tunable Properties. *J. Am. Chem. Soc.* **2003**, *125*, 3896−3900.

(35) Papadopoulou, E. L.; Barberoglou, M.; Zorba, V.; Manousaki, A.; Pagkozidis, A.; Stratakis, E.; Fotakis, C. Reversible Photoinduced Wettability Transition of Hierarchical ZnO Structures. *J. Phys. Chem. C* **2009**, *113*, 2891−2895.

(36) Papadopoulou, E. L.; Zorba, V.; Pagkozidis, a.; Barberoglou, M.; Stratakis, E.; Fotakis, C. Reversible Wettability of ZnO Nanostructured Thin Films Prepared by Pulsed Laser Deposition. *Thin Solid Films* **2009**, *518*, 1267−1270.

(37) Kenanakis, G.; Stratakis, E.; Vlachou, K.; Vernardou, D.; Koudoumas, E.; Katsarakis, N. Light-Induced Reversible Hydrophilicity of ZnO Structures Grown by Aqueous Chemical Growth. *Appl. Surf. Sci.* **2008**, *254*, 5695−5699.

(38) Feng, C. L.; Zhang, Y. J.; Jin, J.; Song, Y. L.; Xie, L. Y.; Qu, G. R.; Jiang, L.; Zhu, D. B. Reversible Wettability of Photoresponsive Fluorine-Containing Azobenzene Polymer in Langmuir-Blodgett Films. *Langmuir* **2001**, *17*, 4593−4597.

(39) Wang, Y.; Li, X.; Wang, N.; Quan, X.; Chen, Y. Controllable Synthesis of ZnO Nanoflowers and Their Morphology-Dependent Photocatalytic Activities. *Sep. Purif. Technol.* **2008**, *62*, 727−732.

(40) Yang, Y. H.; Li, Z. Y.; Wang, B.; Wang, C. X.; Chen, D. H.; Yang, G. W. Self-Assembled ZnO Agave-like Nanowires and Anomalous Superhydrophobicity. *J. Phys.: Condens. Matter* **2005**, *17*, 5441−5446.

(41) Kenanakis, G.; Vernardou, D.; Katsarakis, N. Light-Induced Self-Cleaning Properties of ZnO Nanowires Grown at Low Temperatures. *Appl. Catal., A* **2012**, *411-412*, 7−14.

(42) Kenanakis, G.; Katsarakis, N. ZnO Nanowires on Glass via Chemical Routes: A Prospective Photocatalyst for Indoors Applications. *J. Environ. Chem. Eng.* **2014**, *2*, 1416−1422.

(43) Kenanakis, G.; Pervolaraki, M.; Giapintzakis, J.; Katsarakis, N. The Use of Pulsed Laser Deposited Seed Layers for the Aqueous Solution Growth of Highly Oriented ZnO Nanowires on Sapphire Substrates at 95°C: Study of Their Photocatalytic Activity in Terms of Octadecanoic (stearic) Acid Degradation. *Appl. Catal., A* **2013**, *467*, 559−567.

(44) Zhang, T.; Oyama, T.; Aoshima, A.; Hidaka, H.; Zhao, J.; Serpone, N. Photooxidative N-Demethylation of Methylene Blue in Aqueous TiO_2 Dispersions under UV Irradiation. *J. Photochem. Photobiol., A* **2001**, *140*, 163−172.

(45) Kwon, C. H.; Shin, H.; Kim, J. H.; Choi, W. S.; Yoon, K. H. Degradation of Methylene Blue via Photocatalysis of Titanium Dioxide. *Mater. Chem. Phys.* **2004**, *86*, 78−82.

(46) Houas, A. Photocatalytic Degradation Pathway of Methylene Blue in Water. *Appl. Catal., B* **2001**, *31*, 145−157.

(47) Kenanakis, G.; Katsarakis, N. Chemically Grown TiO2 on Glass with Superior Photocatalytic Properties. *J. Environ. Chem. Eng.* **2014**, *2*, 1748−1755.

(48) Anastasiadis, S. H.; Hatzikiriakos, S. G. The Work of Adhesion of Polymer/wall Interfaces and Its Association with the Onset of Wall Slip. *J. Rheol. (Melville, NY, U. S.)* **1998**, *42*, 795.

(49) Cao, Y.-Q.; Chen, J.; Zhou, H.; Zhu, L.; Li, X.; Cao, Z.-Y.; Wu, D.; Li, A.-D. Photocatalytic Activity and Photocorrosion of Atomic Layer Deposited ZnO Ultrathin Films for the Degradation of Methylene Blue. *Nanotechnology* **2015**, *26*, 024002.

(50) Chen, L. J.; Ma, H.; Chen, K. C.; Fan, W.; Cha, H. R.; Lee, Y. I.; Qian, D. J.; Hao, J.; Liu, H. G. Synthesis and Assembly of Catalytically Active Platinum-Doped Polymer Nanocomposites at the Liquid/liquid Interface. *Colloids Surf., A* **2011**, *386*, 141−150.

(51) Hong, R.; Pan, T.; Qian, J.; Li, H. Synthesis and Surface Modification of ZnO Nanoparticles. *Chem. Eng. J.* **2006**, *119*, 71−81.

(52) Mills, A.; Wang, J. Simultaneous Monitoring of the Destruction of Stearic Acid and Generation of Carbon Dioxide by Self-Cleaning Semiconductor Photocatalytic Films. *J. Photochem. Photobiol., A* **2006**, *182*, 181−186.